

## Supporting Information

### Dry-Milled Microstructure-Controlled Sulfide Electrolytes Enabling Superionic Transport and High-Capacity All-Solid-State Batteries

Ziyu Lu<sup>a, b</sup>, Siwu Li<sup>a</sup>, Lin Li<sup>b</sup>, Ziling Jiang<sup>b</sup>, Long Chen<sup>c, \*</sup>, Miao Deng<sup>b</sup>, Chen Liu<sup>d</sup>, Chuang Yu<sup>a, b, d, \*</sup>

<sup>a</sup> School of Information Mechanics and Sensing Engineering, Xidian University, Xi'an, Shaanxi 710126, P. R. China

<sup>b</sup> School of Chemistry and Chemical Engineering, Huazhong University of Science and Technology, Wuhan 430074, P. R. China

<sup>c</sup> Key Laboratory for Ultrafine Materials of Ministry of Education, School of Chemical Engineering, East China University of Science and Technology, 130 Meilong Road, Shanghai, 200237 China

<sup>d</sup> School of Electrical and Electronic Engineering, Huazhong University of Science and Technology, Wuhan, 430074, P. R. China

\* E-mail: [cyu\\_msubmit@163.com](mailto:cyu_msubmit@163.com)(Chuang Yu), [longchen@ecust.edu.cn](mailto:longchen@ecust.edu.cn) (Long Chen)

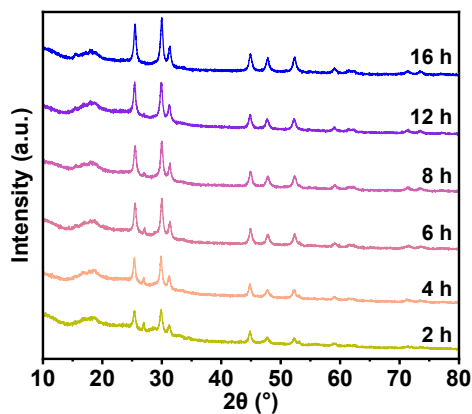


**Fig. S1.** XRD patterns of LPSCB electrolyte at different ball-milling times.

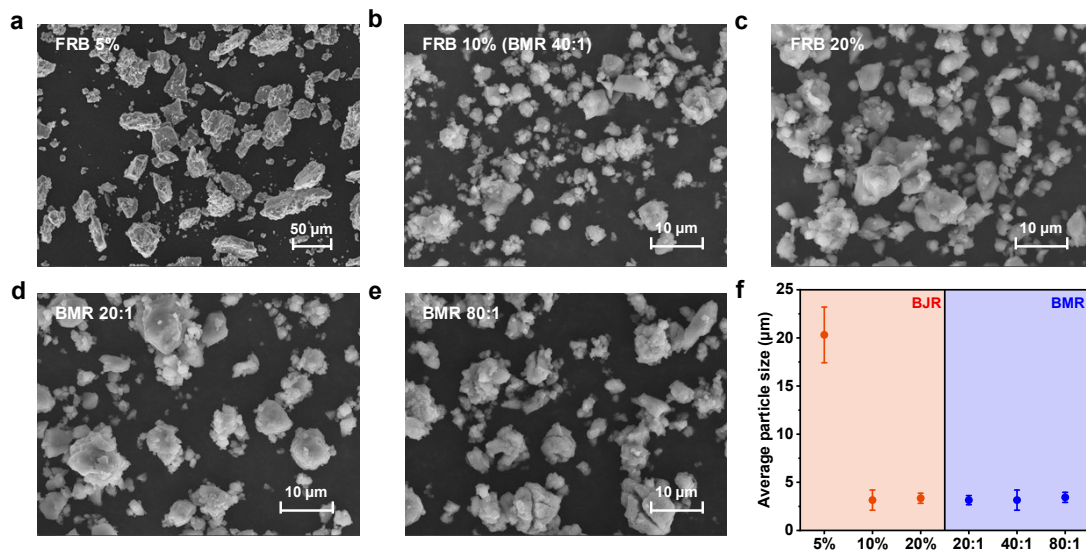


**Fig. S2.** LPSCB electrolytes prepared under different ball milling parameters (a) FRB 5%, b) FRB 10% (BMR 40:1), c) FRB 20%, d) BMR 20:1, and e) BMR 80:1. f) The corresponding particle size distribution diagram.

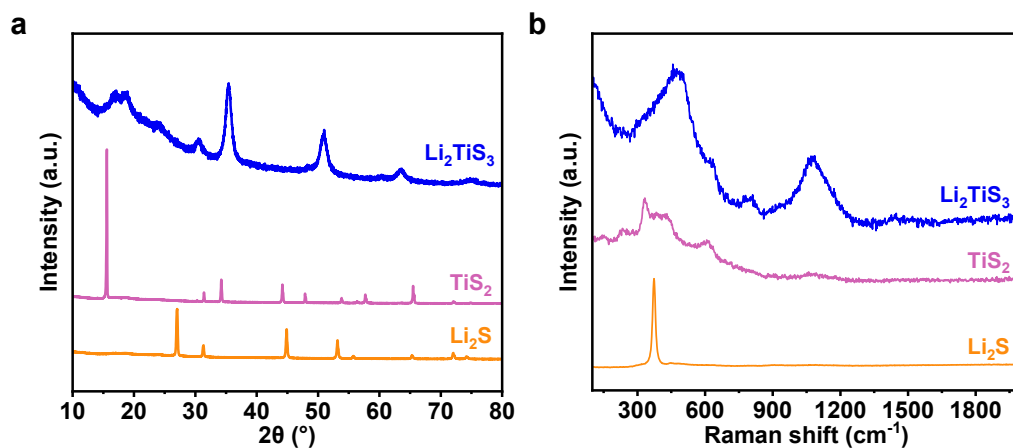


**Fig. S3.** a) XRD pattern and b) Raman spectrum of  $\text{Li}_2\text{TiS}_3$ .

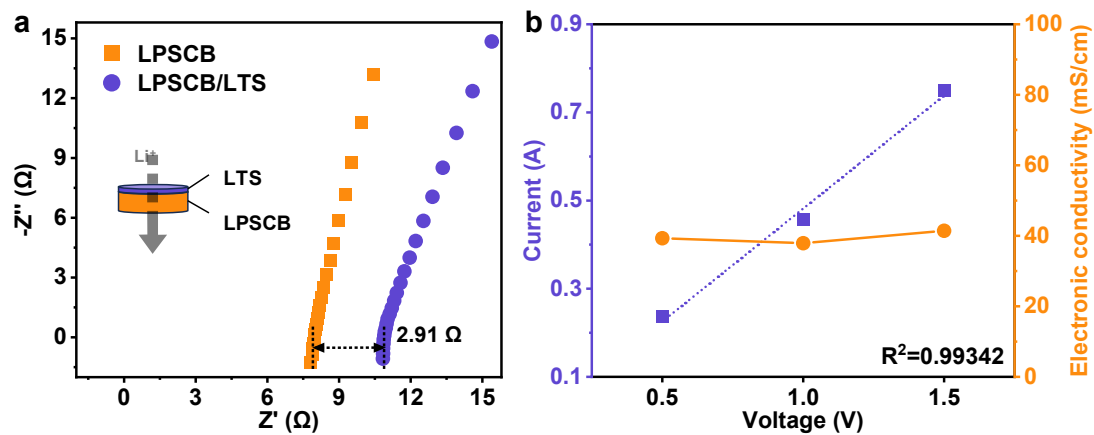


**Fig. S4.** a) Ionic conductivity and b) electronic conductivity of  $\text{Li}_2\text{TiS}_3$ .

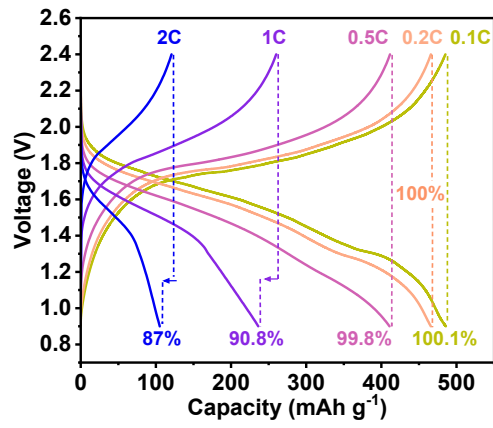


Fig. S5. Charge-discharge curves of LTS/LPSCB/Li-In battery at different rates.

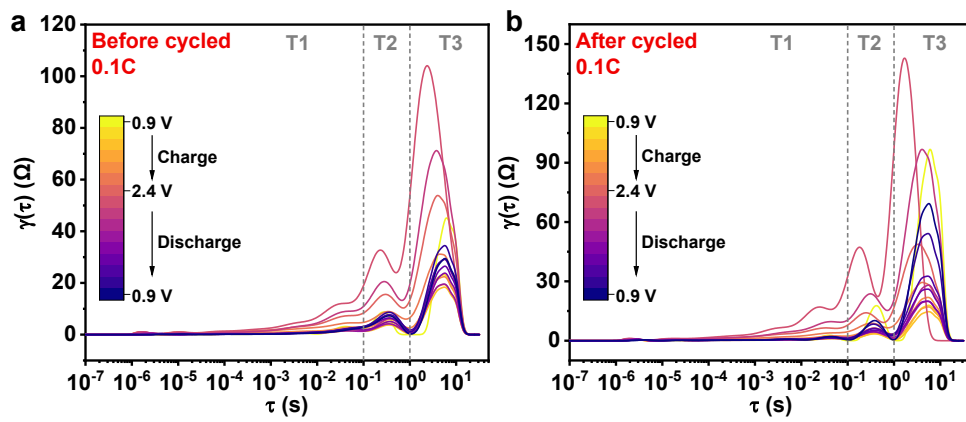
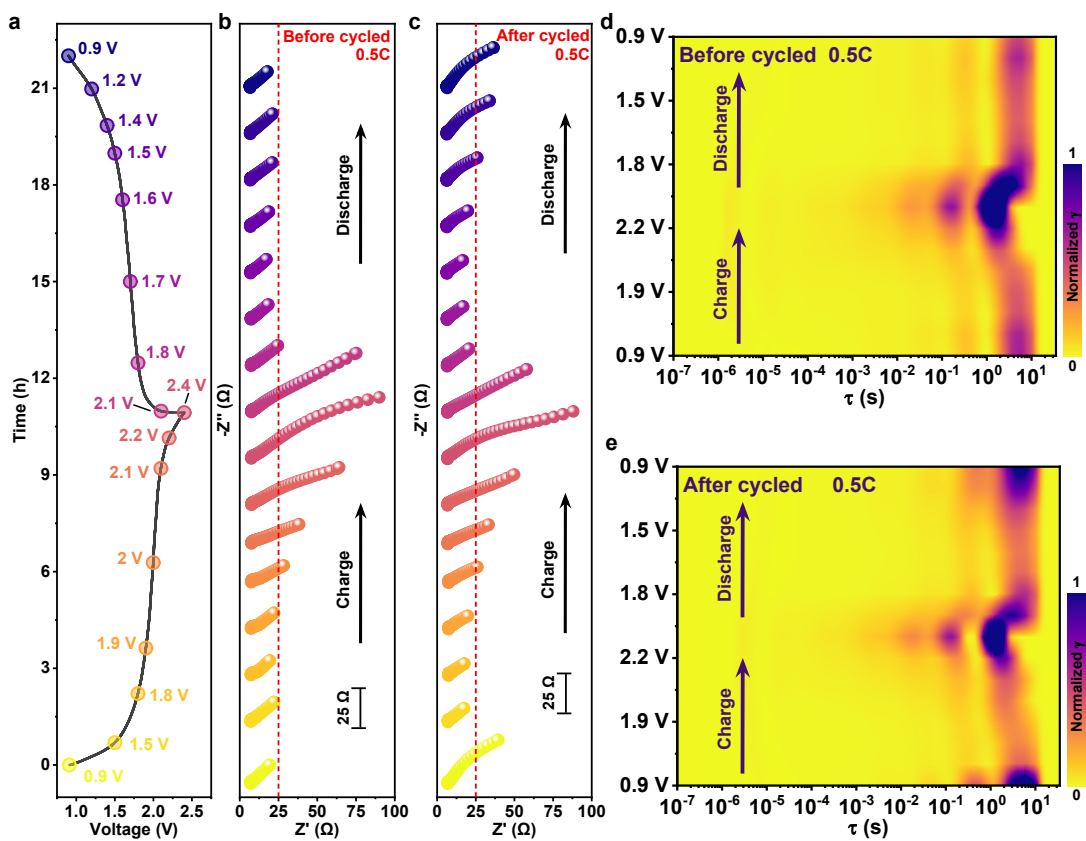
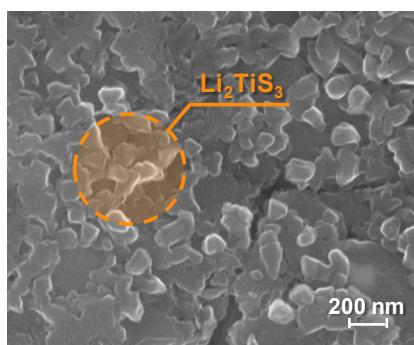


Fig. S6. DRT curves of in-situ impedance for LTS/LPSCB/Li-In batteries a) before and b) after cycling.



**Fig. S7.** Electrochemical evolution process of high-load LTS/LPSCB/Li-In batteries during operation. a) Voltage-time curve of ASSLBs during cycling at 0.5C. b) In-situ EIS spectra of ASSLBs b) before cycling and c) after 20 cycles. d-e) The corresponding 2D intensity mapping of DRT curves of the ASSLBs.



**Fig. S8.** High-resolution SEM image of the cathode region of ASSLBs after cycling.

**Table. S1.** Rietveld refinement parameters for the XRD pattern of LPSCB-5%.

Atom site	x	y	z	Occ.	Wykoff site
Li1	0.30850	0.00020	0.69150	0.4350	48h
Li2	0.25000	0.00220	0.75000	0.0633	24g
S1	0.00000	0.00000	1.00000	0.2150	4a
S2	0.25000	0.25000	0.75000	0.2850	4d
S3	0.11890	-0.11890	0.61890	1.0000	16e
P1	0.00000	0.00000	0.50000	1.0000	4b
Cl1	0.00000	0.00000	1.00000	0.2450	4a
Cl2	0.25000	0.25000	0.75000	0.5550	4d
Br1	0.00000	0.00000	1.00000	0.5400	4a
Br2	0.25000	0.25000	0.75000	0.1600	4d
Space Group: $Pn\bar{3}m$ ; $a=b=c=9.89474\text{\AA}$ ; $\alpha=\beta=\gamma=90^\circ$ ; $V=968.755\text{\AA}^3$					
$R_p=4.11\%$ ; $R_{wp}=6.05\%$ ; $\chi^2=3.392$					

**Table. S2.** Rietveld refinement parameters for the XRD pattern of LPSCB-10%(40:1).

Atom site	x	y	z	Occ.	Wykoff site
Li1	0.30855	0.00025	0.69145	0.4200	48h
Li2	0.25005	0.00225	0.74995	0.0933	24g
S1	0.00005	0.00005	0.99995	0.2110	4a
S2	0.24995	0.24995	0.75005	0.2900	4d
S3	0.11885	-0.11890	0.61890	1.0000	16e
P1	0.00000	0.00000	0.50000	1.0000	4b
Cl1	0.00005	0.00000	1.00000	0.2380	4a
Cl2	0.24995	0.24995	0.75005	0.5620	4d
Br1	0.00005	0.00005	0.99995	0.5350	4a
Br2	0.24995	0.24995	0.75005	0.1650	4d
Space Group: $Pn\bar{3}m$ ; $a=b=c=9.90087\text{\AA}$ ; $\alpha=\beta=\gamma=90^\circ$ ; $V=970.550\text{\AA}^3$					
$R_p=4.76\%$ ; $R_{wp}=6.92\%$ ; $\chi^2=4.611$					

**Table. S3.** Rietveld refinement parameters for the XRD pattern of LPSCB-20%.

Atom site	x	y	z	Occ.	Wykoff site
Li1	0.30845	0.00015	0.69155	0.4100	48h
Li2	0.24995	0.00215	0.75005	0.1033	24g
S1	0.00000	0.00000	1.00000	0.2080	4a
S2	0.25000	0.25000	0.75000	0.2920	4d
S3	0.11895	-0.11885	0.61885	1.0000	16e
P1	0.00000	0.00000	0.50000	1.0000	4b
Cl1	0.00000	0.00000	1.00000	0.2420	4a
Cl2	0.25000	0.25000	0.75000	0.5580	4d
Br1	0.00000	0.00000	1.00000	0.5320	4a
Br2	0.25000	0.25000	0.75000	0.1680	4d
Space Group: $Pn\bar{3}m$ ; $a=b=c=9.89790\text{\AA}$ ; $\alpha=\beta=\gamma=90^\circ$ ; $V=969.680\text{\AA}^3$					
$R_p=4.55\%$ ; $R_{wp}=6.55\%$ ; $\chi^2=3.991$					

**Table. S4.** Rietveld refinement parameters for the XRD pattern of LPSCB-20:1.

Atom site	x	y	z	Occ.	Wykoff site
Li1	0.30860	0.00030	0.69140	0.4400	48h
Li2	0.25010	0.00230	0.74990	0.0533	24g
S1	0.00010	0.00010	0.99990	0.2180	4a
S2	0.24990	0.24990	0.75010	0.2820	4d
S3	0.11880	-0.11900	0.61900	1.0000	16e
P1	0.00000	0.00000	0.50000	1.0000	4b
Cl1	0.00010	0.00010	0.99990	0.2480	4a
Cl2	0.24990	0.24990	0.75010	0.5520	4d
Br1	0.00010	0.00010	0.99990	0.5450	4a
Br2	0.24990	0.24990	0.75010	0.1550	4d
Space Group: $Pn\bar{3}m$ ; $a=b=c=9.90887\text{\AA}$ ; $\alpha=\beta=\gamma=90^\circ$ ; $V=972.892\text{\AA}^3$					
$R_p=4.65\%$ ; $R_{wp}=6.73\%$ ; $\chi^2=4.113$					

**Table. S5.** Rietveld refinement parameters for the XRD pattern of LPSCB-80:1.

Atom site	x	y	z	Occ.	Wykoff site
Li1	0.30840	0.00010	0.69160	0.3800	48h
Li2	0.24990	0.00210	0.75010	0.1567	24g
S1	0.00000	0.00000	1.00000	0.2050	4a
S2	0.25000	0.25000	0.75000	0.2950	4d
S3	0.11900	-0.11880	0.61880	1.0000	16e
P1	0.00000	0.00000	0.50000	1.0000	4b
Cl1	0.00000	0.00000	1.00000	0.2350	4a
Cl2	0.25000	0.25000	0.75000	0.5650	4d
Br1	0.00000	0.00000	1.00000	0.5280	4a
Br2	0.25000	0.25000	0.75000	0.1720	4d
Space Group: ; a=b=c=9.89566Å; $\alpha=\beta=\gamma=90^\circ$ ; $V=969.025\text{\AA}^3$					
$R_p=3.36\%$ ; $R_{wp}=4.95\%$ ; $\chi^2=2.360$					